On the application of the Jensen wake model using a turbulence-dependent wake decay coefficient: the Sexbierum case

Pena Diaz, Alfredo; Réthoré, Pierre-Elouan; van der Laan, Paul

Published in:
Wind Energy

Link to article, DOI:
10.1002/we.1863

Publication date:
2016

Document Version
Publisher's PDF, also known as Version of record

Wind Energy

WIND ENERGY
Wind Energ. 2016; **19**:763–776
Published online 7 May 2015 in Wiley Online Library (wileyonlinelibrary.com). DOI: 10.1002/we.1863

RESEARCH ARTICLE

On the application of the Jensen wake model using a turbulence-dependent wake decay coefficient: the Sexbierum case

Alfredo Peña, Pierre-Elouan Réthoré and M. Paul van der Laan

Department of Wind Energy, Technical University of Denmark, Risø campus, Roskilde, Denmark

ABSTRACT

We present a methodology to process wind turbine wake simulations, which are closely related to the nature of wake observations and the processing of these to generate the so-called wake cases. The method involves averaging a large number of wake simulations over a range of wind directions and partly accounts for the uncertainty in the wind direction assuming that the same follows a Gaussian distribution. Simulations of the single and double wake measurements at the Sexbierum onshore wind farm are performed using a fast engineering wind farm wake model based on the Jensen wake model, a linearized computational fluid dynamics wake model by Fuga and a nonlinear computational fluid dynamics wake model that solves the Reynolds-averaged Navier–Stokes equations with a modified k-ε turbulence model. The best agreement between models and measurements is found using the Jensen-based wake model with the suggested post-processing. We show that the wake decay coefficient of the Jensen wake model must be decreased from the commonly used onshore value of 0.075 to 0.038, when applied to the Sexbierum cases, as wake decay is related to the height, roughness and atmospheric stability and, thus, to turbulence intensity. Based on surface layer relations and assumptions between turbulence intensity and atmospheric stability, we find that at Sexbierum, the atmosphere was probably close to stable, although the stability was not observed. We support these assumptions using detailed meteorological observations from the Høvsøre site in Denmark, which is topographically similar to the Sexbierum region. © 2015 The Authors. *Wind Energy* published by John Wiley & Sons Ltd.

KEYWORDS

atmospheric stability; Sexbierum; turbulence; wake decay coefficient; wake model; wind direction uncertainty

Correspondence

Alfredo Peña, Department of Wind Energy, Technical University of Denmark, Risø campus, Roskilde, Denmark.
E-mail: aldi@dtu.dk

Received 26 May 2014; Revised 30 March 2015; Accepted 16 April 2015

1. INTRODUCTION

The Jensen wake model[1] is popular as an engineering wind turbine wake model for the quantification of the reduction of the wind speed downstream a wind turbine. This is because it was formulated in the early 1980s when only a few wake models were available and is simple, very fast and easy to implement. It is also the base of the Park model[2] that was developed for wind farm calculations for the Wind Atlas Analysis and Application Program (WAsP),[3] which is widely used for the estimation of wind resources. Because of the simplicity of its physical considerations, it is not recognized to be very accurate at predicting wake losses under specific atmospheric inflow conditions, e.g. when compared with wind farm power and meteorological (met) data averaged over a narrow range of wind speeds and directions. It is nevertheless considered to be fairly accurate for predicting wake losses on an annual energy production basis.[4]

Under such specific conditions, the differences between wake simulations and observations can partly be explained by the post-processing methodologies used to reproduce the observed results with a set of model simulations, as pointed out by Gaumond *et al.*[5] and Peña *et al.*[6] A 'wake case' is usually constructed by narrowing the wind speed to its most observed value, often within a range of ± 1 m s^{-1}. Then, different ranges of wind directions are considered, e.g. $\pm 5°$, $\pm 10°$ or $\pm 15°$, and either the observed wind speed or the power deficits are averaged and compared with model simulations.

Now, the question that arises is how does one perform the set of model simulations that can be fairly compared with measured averages? Until recently, we have only been concerned about the improvement of wake models to account for the physics of the turbine–atmosphere interaction, e.g. through computational fluid dynamics (CFD). When a new model or parametrization is developed, it is normally tested against some classic wake cases and generally shows better results compared with those from other known and in many cases simpler models (usually, the Jensen wake model is also used for such purpose). We do not find this tendency very appealing as some of the simulations are still far from being carried out and post-processed in a similar manner as that used when analyzing the wake observations.

The results from Gaumond *et al*.[5] using a wind farm model based on the Jensen wake model, compared with a number of standard wake cases at the offshore wind farm Horns Rev I, were as agreeable as those obtained using more advanced wake models, such as that by Fuga,[7] which is a linearized CFD model that uses the actuator disc (AD) approach, when the post-processing of the results took into account the uncertainty in the wind direction. Gaumond[8] actually showed that for the single and double wake cases at the Sexbierum wind farm, the results from Fuga's model and from a CFD solver of the Reynolds-averaged Navier–Stokes (RANS) equations (EllipSyS)[9] that uses the AD approach and a standard k-ε model are nearly identical; those from the Jensen wake model were not properly post-processed, i.e. the uncertainty in the wind direction was not taken into account, and so the other models seem to *a priori* achieve better results. Further, a wake decay coefficient of 0.075 was used with the Jensen wake model, which is the WAsP-recommended value for onshore wake modeling. Here, we show for the first time

- that this value is nearly two times larger than that obtained for the Sexbierum cases based on a stability-based parametrization of the wake decay and
- that in case information on stability is lacking, one may use the turbulence intensity (TI) instead, as we show, using high-quality observations from Høvsøre (a similar site to Sexbierum in terms of topography), that turbulence and stability are closely related. The stability-based wake decay approach was already successfully evaluated at the Horns Rev I wind farm for a row of 10 turbines and a range of stability conditions.[6]

But why do we try to improve simple engineering wake models? A number of wind farm flow models have been developed over the years using various physical assumptions. While the Jensen wake model represents one of the most simple 'low-fidelity' models, it also remains to be popular in the research and industry wind communities because it can be recalibrated due to its simple wake parametrization. There is always a risk of overfitting while recalibrating models; however, it is important to point out that in wind energy (as an applied science), what ultimately matters is the predictive capability of the wind farm flow models and not the amount of physics or complexity added to them. Simple engineering models offer the possibility of carrying out simulations orders of magnitude faster than higher fidelity ones, allowing us to perform wind farm analysis and optimization. With the advance of probabilistic methods offering ensemble aggregation of models or even multi-fidelity, low-fidelity models can be combined with higher fidelity ones (an example of the latter is CFD RANS) to perform fast and accurate prediction of annual energy production or even wind farm layout optimization.

Here, we first describe the Jensen wake model and a simple method to estimate the wake decay coefficient based either on the height, roughness and atmospheric stability conditions or TI values at a given site (Section 2.1). In Sections 2.2 and 2.3, we briefly introduce the two other wake models used in this study, Fuga and a RANS-based model that uses a modified k-ε turbulence model. Section 3 illustrates the different ways of post-processing the results from the Jensen wake model, e.g. by taking into account the uncertainty in the wind direction. The Sexbierum wake cases are presented in Section 4 and the results of the comparison between these and the wake models in Section 5, followed by the conclusion and discussion.

2. WAKE MODELS

Here, we describe the basics of the three wake models used in this study. For the Jensen wake model, we show the relations between the wake decay coefficient and TI, and the relation between TI and atmospheric stability at the Høvsøre site in Denmark.

2.1. The Jensen wake model

Jensen[1] devised a mass-conserving engineering wake model to estimate the hub height wind speed downstream of a turbine at a distance x, u_2, when subjected to a hub height inflow wind speed u_1 as

$$1 - \frac{u_2}{u_1} = \frac{1 - \sqrt{1 - C_t}}{(1 + k_w\, x/r_r)^2} \tag{1}$$

where C_t is the thrust coefficient, r_r is the rotor radius and k_w is the wake decay coefficient. Figure 1 illustrates that the Jensen wake model assumes the radial speed to be constant within the wake, which expands radially at the rate $k_w\, x$. The term on the left of equation (1) is referred to as the local speed deficit, δ. This model (i.e. the top-hat wake profile shown in Figure 1) is deficient for the far wake but a good approximation in the near wake, e.g. at two rotor diameters downstream.[10]

Wind Energ. 2016; **19**:763–776 © 2015 The Authors. *Wind Energy* published by John Wiley & Sons Ltd.
DOI: 10.1002/we

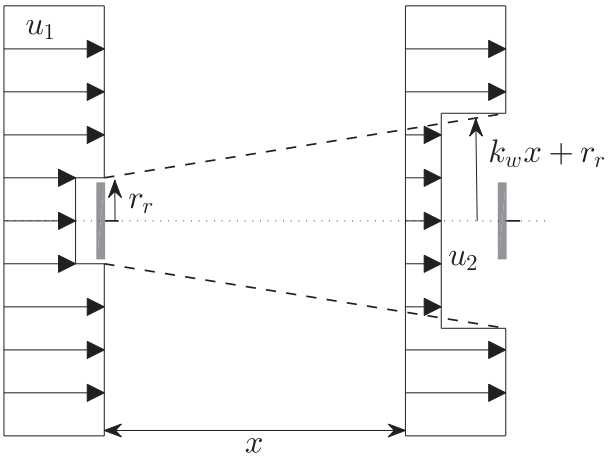

Figure 1. The Jensen wake model concept.

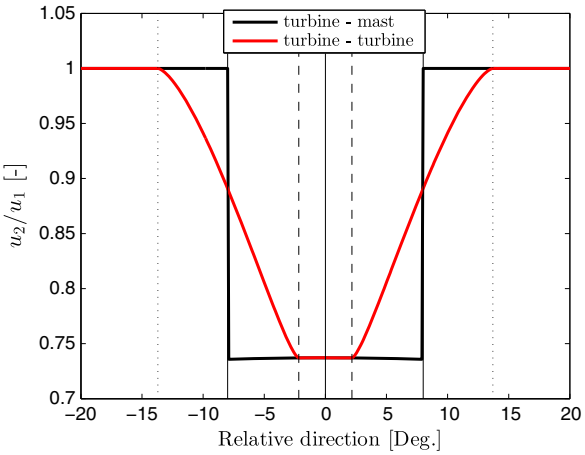

Figure 2. Wind speed ratio of the Jensen-based wind farm model as a function of the relative wind direction. Two cases are illustrated: a wake generated by a turbine and observed by a mast (turbine–mast) and a wake generated by a turbine and observed by a second turbine (turbine–turbine).

2.1.1. Wind farm model.

Within a wind farm, the local wakes are superposed to estimate the speed deficit at the nth turbine, δ_n, and thus, we implement a quadratic sum of the square of the local speed deficits from the Jensen wake model, each represented with the subindex i, as suggested by Katic *et al.*[2] and used in WAsP

$$\delta_n = \left(\sum_{i=1}^{n} \delta_i^2 \right)^{1/2} \tag{2}$$

The speed at the nth turbine, u_n, is then given as $u_n = u_1 \, (1 - \delta_n)$.

When the distance between the local and an upstream turbine is not aligned with the wind's direction, the local turbine could experience a partial wake interaction. The local speed deficit thus needs to be reduced by a factor that depends on the crosswise distance between the wake's center and the local turbine's center, the local turbine's radius and the wake's radius at the downstream position as described by Wan *et al.*[11] This is illustrated in Figure 2, where the wind speed ratio u_2/u_1 from the wind farm model is plotted as the function of the relative wind direction for two cases: first, assuming one turbine only and so u_2 is 'observed' by a point measurement (e.g. a cup anemometer on a met mast) and second, assuming two turbines and so u_2 is 'observed' by the downstream turbine. The simulations are performed at a downstream distance of $5D$, D being the rotor diameter of 30 m using $u_1 = 8$ m s^{-1}, $k_w = 0.038$ and $C_t = 0.75$ for a wide range of relative wind directions with a resolution of 0.1°.

For the 'turbine–mast' case, the downstream wind speed sharply decreases at a given angle and so the ratio u_2/u_1 is similar to the profile of u_2 in Figure 1. Within the wake, u_2/u_1 is not completely constant (u_2 is slightly lower at relative directions other than 0°) because the relative downstream distance decreases slightly with increasing relative direction. For the 'turbine–turbine' case, u_2/u_1 decreases at larger magnitudes of relative direction (compared with the 'turbine–mast' case, u_2/u_1 decreases at $\approx |14°|$) and reaches the maximum deficit at a narrow relative direction range, its size depending on the diameter of the second turbine. When compared with specific wake cases, results from the Jensen wake model might look like those in Figure 2. However, as will be shown in Section 3, such results are misleading, since the characteristics of the processing of the observations are not met by these 'direct' simulations.

2.1.2. The wake decay coefficient.

Until recently, the wake decay was the only adjustable parameter in the Jensen wake model. Peña and Rathmann[12] suggested the relation $k_w = u_{*free}/u_{hfree}$, where u_{*free} is the free friction velocity and u_{hfree} the free hub height wind speed, for the estimation of the value of the wake decay coefficient in models based on the Jensen wake model, based on Frandsen's findings.[13] The results of such a relation are much smaller k_w values compared with those commonly used (e.g. WAsP's default k_w value for an onshore site is 0.075). Therefore, we believe that most of the work carried out so far using Jensen's approach tends to underestimate the wake losses when performed over terrain with low roughnesses. Further, assuming that the aforementioned relation for k_w is correct, we can relate k_w to atmospheric stability and TI. Using the surface layer theory,[14] one can find that within the surface layer over flat and homogeneous terrain, the following holds,

$$u_{hfree} = \frac{u_{*free}}{\kappa}\left[\ln\left(\frac{h}{z_o}\right) - \psi_m(h/L)\right] \tag{3}$$

where κ is the von Kármán constant (≈ 0.4), h the hub height, z_o the surface roughness length and $\psi_m(h/L)$ the local atmospheric stability correction, which is estimated at a given height (in this case at hub height), for the specific stability condition (measured by the Obukhov length L[15]).

The surface layer diabatic wind profile in equation (3) is only valid within the surface layer accounting for the lowest ≈10% of the atmospheric boundary layer. Therefore, its ability to accurately predict winds at turbine operating heights depends on the boundary layer height (BLH); for unstable and neutral conditions in middle latitudes, the BLH is about 500 m or higher, thus, equation (3) is valid at least for the first 50 m from the ground. On the other hand, under stable conditions, the BLH might be as low as 100 m for such latitudes; thus, equation (3) might be valid within the first 10 m only. This means that surface layer expressions can be used within a broad range of stability conditions for small to medium size wind turbines, but should carefully be applied for large turbines or extended to account for other parameters such as BLH.[16,17] Equation (3) has however been found to be valid over nearly flat and homogeneous terrains up to ≈40–60 m in very stable conditions and at heights above 100 m in neutral and unstable conditions.[17,18]

Assuming equation (3) is valid at the turbine height, k_w can be expressed as

$$k_w = \kappa\left[\ln\left(\frac{h}{z_o}\right) - \psi_m(h/L)\right]^{-1} \tag{4}$$

The standard deviation of the free stream flow (in this case at hub height), $\sigma_{u_{hfree}}$, can be assumed as a function of the free friction velocity of the form, $\sigma_{u_{hfree}} \approx A\, u_{*free}$.[19] The parameter A depends on atmospheric stability and BLH. Here, we assume that it is constant ($A \approx 2.5$) for practical reasons as $A\,\kappa \approx 1$. Such value is close to the average of estimates of A reported by Panofsky and Dutton[19] based on a number of campaigns over flat terrain under neutral conditions ($A = 2.39 \pm 0.03$).* We test our assumption regarding A with data from a wide range of stability conditions in the next section.

Defining the TI as $\mathrm{TI} = \sigma_u/u$, it is easy to demonstrate

$$\mathrm{TI} \approx \left[\ln\left(\frac{z}{z_o}\right) - \psi_m(z/L)\right]^{-1} \tag{5}$$

$$k_w \approx 0.4\,\mathrm{TI}_h \tag{6}$$

where z is the height above ground and TI_h the hub height TI, which can be found by evaluating equation (5) with $z = h$. These two relations are only valid for flat and homogeneous terrain and within the surface layer, thus, under stable conditions, in particular when $z/L \geq 1$, large deviations can occur when estimating wind and turbulence characteristics outside of this layer.[20] Unfortunately, it is difficult to observe, account for and estimate the BLH because of the dynamics of the atmosphere. Further, there are other phenomena, such as baroclinity, influencing the wind profile higher up.[21]

*In Panofsky and Dutton,[19] A is related to the along-wind speed component that we assume equal to the magnitude of the wind speed, which is a fair assumption within the surface layer only.

Wind Energ. 2016; **19**:763–776 © 2015 The Authors. *Wind Energy* published by John Wiley & Sons Ltd.
DOI: 10.1002/we

2.1.3. Turbulence intensity and atmospheric stability—onshore observations.

In Section 2.1.2, k_w and TI were related to atmospheric stability through assumptions about the behavior of the vertical wind profile and the turbulence close to the ground. The question is whether these assumptions can be tested and validated. We first illustrate the relation between u_* and σ_u in Figure 3. The data are from met observations from an onshore mast located at Høvsøre, a flat farmland area in western Denmark, where atmospheric stability and turbulence have continuously been monitored over the last $\approx$ 9 years. Details about the mast, the measurements and the site are provided in many studies.[17,20,22–25] We select 10 min cup and sonic anemometer observations of the mean and standard deviation of the wind speed and of the friction velocity at 40 m recorded over the last 8 whole years. The data are for easterly winds, where the upstream conditions are nearly homogeneous, under all conditions of atmospheric stability and when wind speeds are within the range of 4–25 m s^{-1} that enables most wind turbines to extract energy from the wind. It is observed that $\sigma_u \approx 2.5\, u_*$ with a rather high linear correlation. Similar results are found when using data from the instruments at a height of 10 m.

Equation (5) indicates how the TI relates to the height, roughness and atmospheric stability. Figure 4 illustrates its validity and that of the related assumptions using the observations at 40 m from the Høvsøre site within a wide range

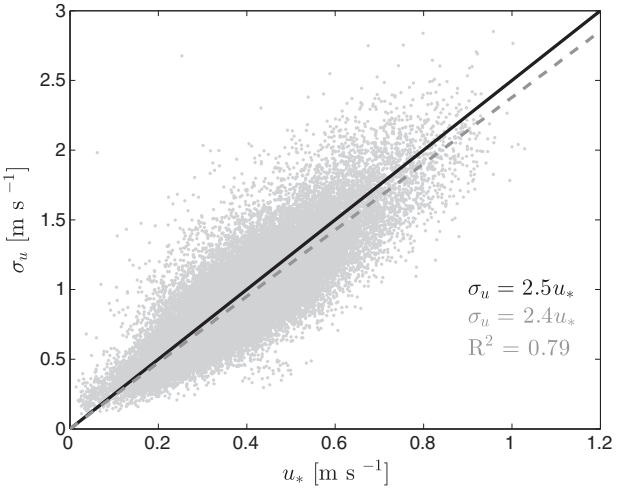

Figure 3. Observations (in markers) of the standard deviation of the wind speed (σ_U) as function of the friction velocity (u_*) at a height of 40 m at Høvsøre, Denmark. The lines correspond to the relation $\sigma_U = A\, u_*$; the solid black line for $A = 2.5$ and the gray dashed line for the linear regression through the origin of the observations. R^2 is the Pearson's linear correlation coefficient.

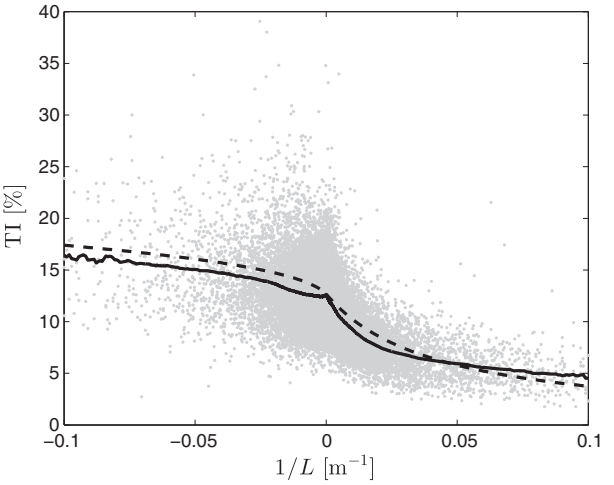

Figure 4. Observations (in markers) of the turbulence intensity (TI) as function of atmospheric stability at a height of 40 m from Høvsøre, Denmark. A moving average of the observations is shown with the solid line and the estimate using equation (5) with the dashed line.

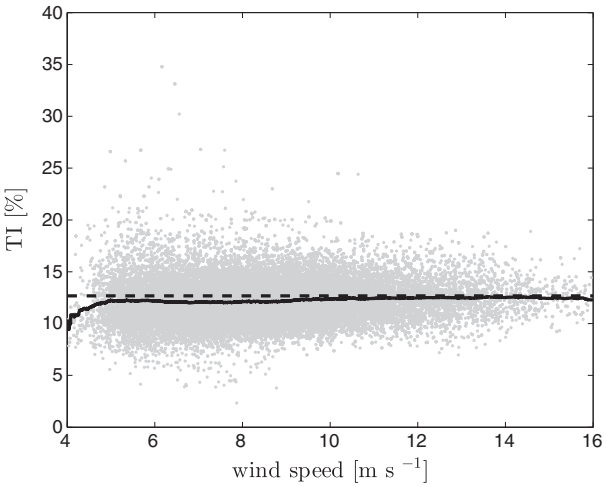

Figure 5. Near-neutral observations (in markers) of turbulence intensity (TI) as a function of wind speed at 40 m at Høvsøre, Denmark. A moving average of the observations is shown with the solid line and the estimate using equation (5) with the dashed line.

of stabilities, $-0.1\ \mathrm{m}^{-1} \leq 1/L \leq 0.1\ \mathrm{m}^{-1}$. On a long-term basis,[†] the roughness at Høvsøre for easterly upstream conditions is about 0.015 m (it slightly increases and decreases in summer and winter, respectively) and so we use this value to estimate TI from equation (5). To estimate ψ_m, we use the form in Gryning *et al.*[26] for unstable conditions, i.e. $\psi_m(z/L) = (3/2)[(1 + a + a^2)/3] - \sqrt{3}\arctan[(1 + 2a)/\sqrt{3}] + \pi/\sqrt{3}$, where $a = (1 - 12z/L)^{1/3}$, and $\psi_m = -4.7z/L$ for stable ones. Both forms were previously used at Høvsøre in Gryning *et al.*[26] for evaluating wind profile models.

The TI estimation using equation (5) clearly follows the behavior of the moving average of the observations, i.e. higher and lower TIs are found for unstable and stable conditions, respectively. However, the observations are scattered, particularly under near-neutral and unstable conditions. This is partly due to the scatter of the observations in Figure 3 and to the accuracy of the diabatic wind profile in equation (3) in predicting the wind speed at this height at Høvsøre. The differences between the moving average and the TI estimation are partly due to the ψ_m forms used and the accuracy of the estimations of L.

The estimate of TI under neutral conditions $1/L \approx 0\ \mathrm{m}^{-1}$ agrees well with the value from the observations. From the same data, we select near-neutral conditions ($|L| \geq 1000$ m) to analyze the dependency of TI on wind speed. Figure 5 illustrates the measurements of TI as function of the wind speed for the height of 40 m, where it is shown a nearly constant behavior with wind speed as expected from the observations. The average TI for the applied moving window is 12.22% for the height of 40 m, which is nearly the same value as that estimated theoretically using equation (5) with $\psi_m = 0$ and $z_o = 0.015$ m, i.e. 12.68%. Similar agreement is found when using observations from the instruments at the height of 10 m.

2.2. Fuga's model

Fuga is a linearized flow solver based on the steady-state RANS equations, currently only applicable to flat and homogeneous terrain. In this model the flow is assumed to be incompressible and lid driven at the chosen inversion height. It uses a simple eddy viscosity turbulence closure and the AD approach. The description of the model and its evaluation with a number of wind farm datasets can be found in Ott *et al.*[7]

2.3. RANS using a modified *k*-ε turbulence model

The AD RANS simulations are carried out in EllipSys3D[9] using a modified k-ε turbulence model, namely, the k-ε-f_P model.[27] The k-ε-f_P model delays the wake recovery compared with the standard k-ε model by introducing a variable eddy viscosity coefficient C_μ. The variable part of C_μ is described by a simple scalar function f_P that depends on the local velocity gradients. Typically, f_P is unity in the logarithmic solution, while it is smaller than one for regions with high velocity gradients. The AD RANS setup including the k-ε-f_P model has been successfully tested for single wakes,[27] double wakes[28] and complete wind farm simulations.[29]

[†]Here, long term refers to measurements performed for at least 1 year.

Wind Energ. 2016; **19**:763–776 © 2015 The Authors. *Wind Energy* published by John Wiley & Sons Ltd.
DOI: 10.1002/we

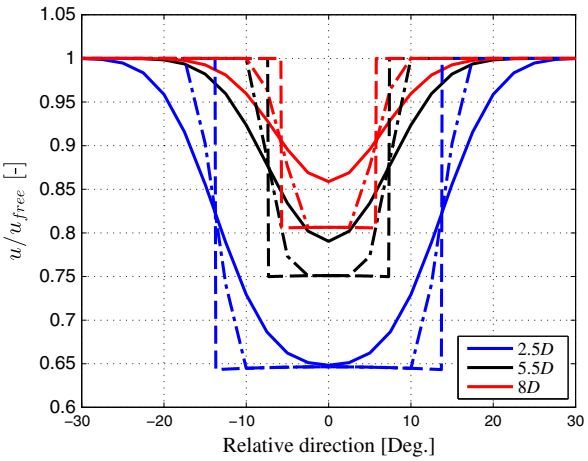

Figure 6. Wind speed ratio from the Jensen wake model as a function of the relative wind direction for the 'turbine–mast' case at three downstream distances. Dashed, dash dotted and solid lines show the results from the 'direct', 'average' and 'uncertainty' simulation results, respectively (see corresponding text for details).

3. COMPARING WAKE SIMULATIONS WITH OBSERVATIONS

How do we simulate an observed wake condition? Ideally, we should aim to simulate each condition that was observed during the particular wake experiment/dataset. However, most wake measurements, as most met measurements, are normally stored as averages (of different types of parameters) over 10 min intervals (hereafter referred to as means). In a nearly ideal situation, one could try to simulate each mean condition, as shown in Peña *et al.*,[6] and then the evaluation could be performed by estimating the difference between simulations and observations, e.g. through the mean square error. However, this is a computationally expensive approach for advanced models, particularly those based on CFD.

Unfortunately, most wake cases are 'constructed' by averaging such means based on a specific range of wind directions, wind speeds, turbulence intensities and atmospheric stabilities (the last two in the best of the cases).[‡] This is rather problematic as wake data are either scarce or of poor quality and so the means do not distribute equally within such ranges and the wake datasets do not normally provide parameters, such as the standard deviation of the wind direction or that of the atmospheric stability, with which we can discern such distributions.

Further, within the 10 min interval, the wind speed follows a distribution that we normally ignore as we can somehow characterize it through the TI. Also, and most important, is that the wind direction is inherently uncertain. This uncertainty can be divided into two parts: the natural variability of the wind direction due to atmospheric turbulence and the measurement error uncertainty. A part of the wind direction variability is taken into account by the wake expansion in the model (the wake decay coefficient) but another important part is related to the spatial and temporal de-correlation of the wind direction between the measurement and the turbine locations, large-scale phenomena such as meandering and sensor inaccuracy and uncertainty among others. Gaumond *et al.*[5] assumed these additional sources of uncertainty to follow a Gaussian distribution and found a dramatic change in the ensemble results.

Using the same parameters as those in Section 2.1.1, we perform simulations using the Jensen wake model of the 'turbine–mast' case at different downstream distances: 2.5D, 5.5D, and 8D. Figure 6 illustrates three different results for each downstream distance, and as expected, the further the downstream distance the higher the ratio u_1/u_2 and the narrower the wake. The first set of results are 'direct' simulation outputs (with a direction resolution of 0.1°) without further post-processing and so their shape is the same as that in Figure 2 for the 'turbine–mast' case. The second set (referred to as the 'average' result) is found by assuming that the observed wake deficits (i.e. the mean observation over a 10 or 30 min interval) actually have a resolution of 0.5° and so the wake case is produced by averaging them over directions between ±2.5° (assuming they are equally distributed over such size, thus 11 deficits are averaged within ±2.5° relative wind directions). The third set (referred to as 'uncertainty' result) is similar to the second one, except that before averaging them within the ±2.5° range, we partly account for the uncertainty in the direction by assuming that within the interval used for estimating the mean, the direction is Gaussian distributed with a standard deviation σ (in this case 5°). Thus, a Gaussian distribution is constructed for each of the 0.5° wake observations and the wake deficits are Gaussian-weighted within the range ±3 σ using the simulations with a resolution of 0.1°. The third approach is equivalent to a forward propagation of

[‡] The result of this average will here be referred to as ensemble mean.

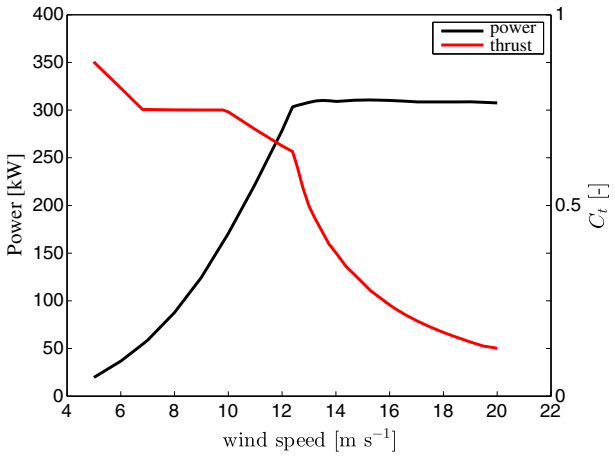

Figure 7. Power and thrust coefficient curves of the Holec WPS-30 wind turbine.[30,31]

the uncertainty of the wind direction that is Gaussian distributed. Another way to account for the uncertainty of the wind direction (but computationally more expensive) is to perform an ensemble of Monte-Carlo simulations, where the wind direction can be sampled from a normal distribution and subsequently averaging the result.

The 'average' result is already different from the 'direct' one. It shows a wind speed ratio that closely follows a tapered shape with wind speed deficits (for the three downstream distances) as large as those from the 'direct' outputs. The 'uncertainty' result is, as the Gaussian distribution, bell-shaped with wind speed ratios less than 1 at higher absolute relative directions (since some part of the Gaussian-weighted wind direction is still wake affected). The maximum wind speed deficits become close to those of the direct outputs the closer the distance to the turbine.

4. THE SEXBIERUM CASE

Sexbierum is, as the region, the name of an onshore wind farm about 4 km from the Dutch North Sea. It consists of 18 pitch-regulated, variable speed, Holec WPS-30 wind turbines with a hub height of 35 m, a rotor diameter of 30.1 m and a rated power of 310 kW. The thrust coefficient is constant ($C_t = 0.75$) within the range 6.8–10 m s^{-1}. The terrain around the wind farm is flat and rather homogenous characterized by grassland. The layout is a 6×3 array and for our purpose, we are going to use the experimental data from the single and double wake measurements reported by Cleijne.[30,31] Figure 7 shows the power and thrust coefficient curves of the turbines at Sexbierum.

In the single wake case, the wind speed was measured during six months at masts located $2.5D$, $5.5D$ and $8D$ downstream of a turbine, when this was facing free stream conditions. For the double wake case, the measurements were performed during three months based on the power of a third turbine (P36) downstream of two others at $5D$ and $10D$ (P38). Data were analyzed when the 'first' turbine faced free stream conditions. The details on the mast and turbine instrumentation, data and averaging methods are given in Cleijne.[30,31] There is no information related to the error or uncertainty of the recorded data. Both cases present data of either observed wind speed (single case) or power ratios (double case) as function of the observed relative wind direction within a range of $\pm 30°$ at a resolution of 2.5°. The wind speed observations were distributed within the range of 5–10 m s^{-1}.

4.1. Turbulence intensity and atmospheric stability

Cleijne[30,31] provided the values of the observed free stream TI (9.5% for both cases) and the upstream roughness (0.049 and 0.045 m for the single and double wake cases, respectively) at Sexbierum. However, no information related to atmospheric stability is provided.

As shown in Section 2.1.3, for a flat and nearly homogenous site, equation (5) reasonably predicts the TI for a given height and roughness under neutral conditions. Assuming at first that the topographical conditions of the Sexbierum area are 'similar' to those of Høvsøre (both sites are nearly flat and based on the Corine Land Cover database[§] the two areas correspond to the arable land and permanent crops category) and that the conditions of the experiments at Sexbierum were

[§]http://www.eea.europa.eu/data-and-maps/data/corine-land-cover-2006-raster-3

Wind Energ. 2016; **19**:763–776 © 2015 The Authors. *Wind Energy* published by John Wiley & Sons Ltd.
DOI: 10.1002/we

nearly neutral, the TI is estimated as $\approx 15\%$ using equation (5) for both wake cases, i.e. close to twice the value from the aforementioned reports. A very possible explanation for the mismatch between observed and estimated TI is the influence of atmospheric stability; from equation (5), the conditions should have to be stable in order to be close to the observed TI. Using the form $\psi_m = -4.7z/L$[14] and equation (5) with $z = 35$ m, TI $= 9.5\%$ and $z_o = 0.049$ m, L is estimated to be 42 m. Another possibility is an inaccurate roughness length estimation in Cleijne's analysis and so there is a range of stabilities and roughnesses that can produce the same TI following equation (5). Because of the mismatch and range of possibilities, for the model simulations based on the atmosphere-dependent wake decay coefficient, we use equation (6) to determine k_w from the observed TI at Sexbierum ($k_w = 0.038$).

5. RESULTS

For both wake cases, we assume the influence from the nearby turbines at Sexbierum to be negligible. So only one and three turbines are modeled, respectively (this is why the layout of the wind farm is not important). Also, for both cases, simulations are performed using a hub height wind speed u_h of 8 m s^{-1}, since Cleijne[30,31] reported that the wind speeds were mostly within the range of 7–9 m s^{-1}. Simulations are carried out using the wind farm model described in Section 2.1.1 with $k_w = 0.038, 0.061$ and 0.060 (the last two are derived using equation (4) assuming neutral conditions and the roughness values from the single and double wake experiments reported earlier, which are close to the default WAsP value) and for a broad range of relative wind directions ($\pm 60°$) with a resolution of $0.1°$. The observations are reported every $2.5°$, and thus, we post-process the results following the steps described in Section 3 related to the 'uncertainty' result. We also show the 'direct' results, i.e. those without any post-processing for completeness.

Results using Fuga's model and RANS using the k-ε-f_P model are also presented. Fuga's inputs are $u_h = 8$ m s^{-1}, roughness length (the values from Cleijne[30,31] are used) and inversion height (we choose 200 m, and the model results are rather insensitive to this input for the Sexbierum wind farm as the flow is lid driven). For the RANS-based one, we need $u_h = 8$ m s^{-1} and TI $= \sqrt{2/3k}/u_h = 0.095$ and, z_o is set so that we obtain the same TI at hub height using TI $= \kappa\sqrt{2/3}/\left[\ln(h/z_o)C_\mu^{1/4}\right]$, i.e. $z_o = 0.009$ m. Note that C_μ is 0.03 and cannot be adapted to obtain the desired TI in the k-ε-f_P model because the behavior of the f_P function changes in an unphysical manner with C_μ, as discussed in van der Laan *et al.*[27]

5.1. Single wake

Observations and simulation results of the Sexbierum single wake case at the three different downstream distances are shown in Figure 8. 'Direct' and 'uncertainty' simulation results are shown for two wake decay coefficients, and the post-processing is carried out using two σ values.

Results from 'direct' simulations show different shapes for the wind speed ratio when compared with the observations. Those using the lowest k_w-value show the highest speed deficits and the narrowest wakes, as expected. It is important to point out that the results based on Jensen's approach have traditionally been close to the simulations shown with the black dotted lines as uncertainty in the wind direction was not usually considered, and the k_w was often assumed to be close to the WAsP-recommended onshore value of 0.075. With the 'direct' simulation results, it is possible to isolate the decrease in wind speed ratio and wake width due to the decrease in the k_w-value; for the three downstream distances, u_2/u_1 is reduced by 7–8% and the wake width (given by $2\tan(k_w)$) by $2.63°$.

Simulation results using $\sigma = 2°$ (left frames) show lower wind speed ratios compared with those using $\sigma = 5°$ (right frames), as expected. So, they are generally closer to the observations. The shapes between the simulations and observations are also closer to the results obtained using the lower σ value. These results, particularly those using $\sigma = 5°$, are closer in shape to the results using Fuga's model. However, the maximum speed deficit predicted by Fuga's model is clearly much lower than that of the observations, any of the Jensen-based simulations and the k-ε-f_P model for the three downstream distances. Neither the results from Fuga's model nor those from the k-ε-f_P model are post-processed to account for the uncertainty in the wind direction, and by doing so, we will obtain even lower speed deficits with regard to the Sexbierum measurements.

Simulation results using $\sigma = 2°$ nearly reach the wind speed ratio of the 'direct' result for the three downstream distances, and the wake width of the 'uncertainty' results is $\approx 14°$ wider than that of the 'direct' ones. For $\sigma = 5°$ at $5.5D$ and $8D$, u_2/u_1 is lower and the wake $\approx 32°$ wider than the results of the 'direct' simulations. The difference between the Jensen-based simulations and observations at $2.5D$ is either due to the ability of the wake model itself (not due to the validity of the assumptions in equations (3)–(6)) or due to the quality of the observations. Assuming that the observed wind speed was actually 8 m s^{-1}, k_w needs to become 0 in order to get such a low wind speed ratio.

Unfortunately from the Sexbierum campaigns, there is no information with which we can derive σ or approximate the spread of the additional uncertainty in wind direction, which was not taken into account by the wake expansion. However,

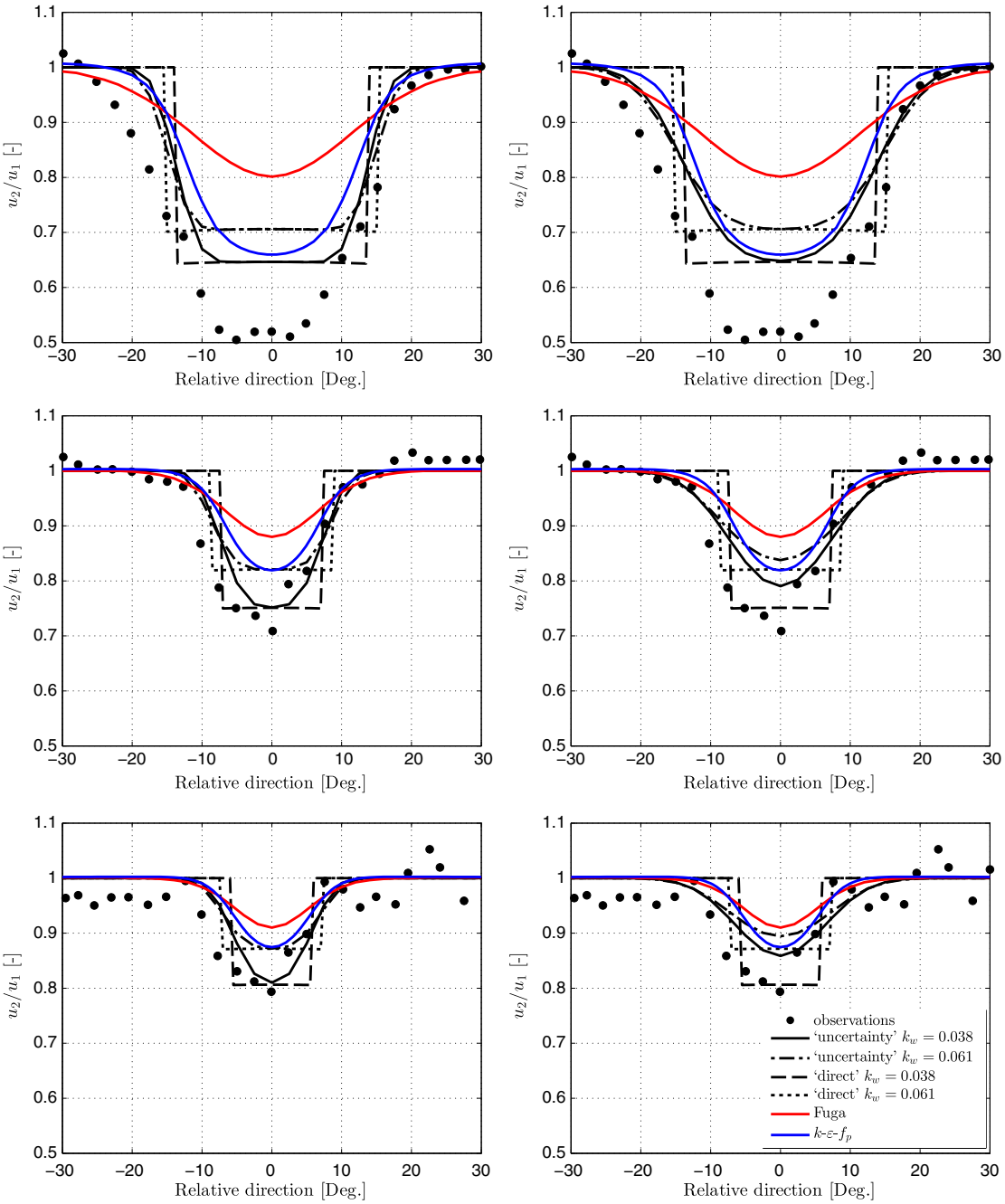

Figure 8. Single wake for three downstream distances at Sexbierum: 2.5D (top frames), 5.5D (middle frames) and 8D (bottom frames). Model results are shown with lines and data from Sexbierum with markers. 'Uncertainty' results from the Jensen-based wake model are post-processed using $\sigma = 2^{\circ}$ (left frames) and $\sigma = 5^{\circ}$ (right frames).

we can use wind direction observations from the Høvsøre site to obtain an idea of the variability of the wind direction within a 10 min interval for conditions 'similar' to those at Sexbierum.

We select fast measurements (20 Hz) from a sonic anemometer located at 40 m on the Høvsøre mast (the closest to the hub height at Sexbierum) that are close to the wind conditions at Sexbierum in terms of wind speed, the suggested atmospheric stability (i.e. $L = 42$ m that is derived by estimating $\psi_m(z/L)$ from equation (5) using the observed values of TI and z_o observed at Sexbierum), and TI (derived using equation (5) using the roughness at Høvsøre and the stability, $L = 42$ m, at Sexbierum). We restrict the analysis to the east sector.

Wind Energ. 2016; **19**:763–776 © 2015 The Authors. *Wind Energy* published by John Wiley & Sons Ltd.
DOI: 10.1002/we

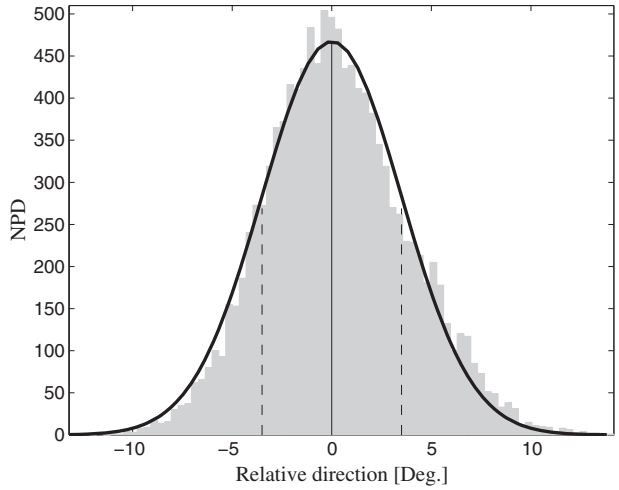

Figure 9. Normalized probability distribution (NPD) of the relative direction observed at Høvsøre for a typical 10 min interval similar to the conditions at Sexbierum. The observations are shown in the histogram with the gray bars, the normal distribution with a solid black line and with dashed lines the $\pm\sigma$ values (3.5°).

Table I. Root mean square error of the wind speed ratio (for the single wake cases) and of the power ratio (for the double wake cases) when comparing model results with the data from Sexbierum.

Model	Single 2.5D	Single 5.5D	Single 8D	Double
Jensen ($\sigma = 0°, k_W = 0.038$)	0.108	0.059	0.049	0.060
Jensen ($\sigma = 0°, k_W = 0.060$)	0.110	0.048	0.049	0.085
Jensen ($\sigma = 2°, k_W = 0.038$)	0.091	0.035	0.041	0.067
Jensen ($\sigma = 2°, k_W = 0.060$)	0.111	0.045	0.045	0.095
Jensen ($\sigma = 5°, k_W = 0.038$)	0.094	0.039	0.041	0.105
Jensen ($\sigma = 5°, k_W = 0.060$)	0.117	0.052	0.048	0.128
Fuga	0.187	0.073	0.056	0.136
k-ε-f_P	0.115	0.053	0.050	0.131

Figure 9 shows an example of such variability within a 10 min interval where the normal distribution is a least squares fit of the histogram of observed relative directions resulting in $\sigma = 3.5°$ (this is the typical value found from the analysis performed for about eighty 10 min histograms of wind direction recorded by the sonic anemometer). As expected, the observed variability is larger than the value that correlated better with the wake observations at Sexbierum ($\sigma = 2°$) because the observed variability should be close to that obtained when adding the effect of the wake expansion and the simulated additional uncertainty in wind direction.

Table I summarizes the results of comparing quantitatively the Sexbierum data with the models in terms of the wind speed ratio. For the three single wake cases, the Jensen-based wake model using $\sigma = 2°$ and $k_w = 0.038$ shows the lowest root mean square error, whereas Fuga's model the highest.

5.2. Double wake

Observations and simulation results of the Sexbierum double wake case are shown in Figure 10. 'Direct' and 'uncertainty' simulation results are shown for two wake decay coefficients, and the post-processing is also carried out using two values of σ.

Similar to the single wake case, 'direct' simulation results do not show the bell-shaped characteristic of the observations, although in this case, the power ratio does not sharply decrease but follows a close to tapered shape due to the superposed wakes. The lowest power deficit is found when using a value of k_w close to that of WAsP and the highest when using $k_w = 0.038$, which matches well that of the observations. Again, results of models using Jensen's approach have traditionally resembled these 'direct' outputs, particularly the case with $k_w = 0.060$. The effect of decreasing k_w is a decrease in the power ratio by 39% with nearly no change in the wake's maximum width.

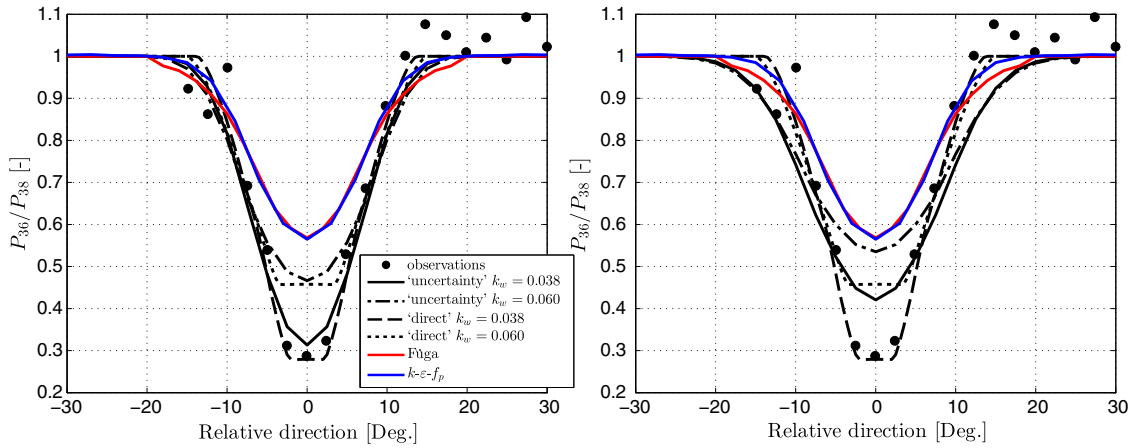

Figure 10. Double wake at Sexbierum. Model results are shown with lines and data from Sexbierum with markers. 'Uncertainty' results from the Jensen-based wake model are post-processed using $\sigma = 2^\circ$ (left frame) and $\sigma = 5^\circ$ (right frame).

Also, similar to the single wake case, the simulation results using $\sigma = 2^\circ$ show the lowest power ratio compared with those using $\sigma = 5^\circ$, as expected. Thus, they are generally closer to the observations and to the 'direct' result using the low k_w-value. In this case, one clearly sees the effect of the uncertainty in relative wind directions other than zero because wakes are simulated between $\pm 20^\circ$ for the $\sigma = 5^\circ$ case. No wake is shown at similar relative wind directions for the $\sigma = 2^\circ$ case. The power ratio curve of the simulation using $\sigma = 2^\circ$ is very close to that of the observations. Results based on the Jensen model are much closer to the observed power ratio when compared with those of Fuga's model and those of the k-ε-f_P model, which clearly underpredict the maximum power deficit as for the single wake cases. Table I shows that all in all, the best results for the double wake cases are obtained when using the 'direct' result from the Jensen-like model with the lowest wake decay coefficient.

In the single wake case, there is a large difference between the results from Fuga's model and RANS using the k-ε-f_P model, while both models show a similar power deficit in the double wake case. This can be explained as follows. The employed turbulence model in Fuga is not valid in the near wake, where velocity gradients are high. On the contrary, the k-ε-f_P turbulence model can handle the high velocity gradients because the f_P function locally limits the eddy viscosity. Further downstream, the difference between the models reduces because the turbulent kinetic energy is increased, and the velocity gradients are not as high as in the near wake of the first wind turbine. Hence, the third wind turbine in the double wake case observes a similar inflow velocity for both models, which translate to a comparable power deficit. A similar observation is made by van der Laan *et al.*,[29] where a near wake invalid turbulence model (the standard k-ε model) only shows differences in terms of the power deficit with the k-ε-f_P model for the first wind turbines in a row of a wind farm.

The neutral RANS simulations underpredict the measured velocity and power deficits because the wake measurements were most likely conducted in a stable atmospheric boundary layer, as discussed in Section 4.1. The comparison with the measurements can be improved if stability is modeled in the RANS simulations, i.e. a Bouyant production/destruction term is added to the transport equation of turbulent kinetic energy that suppresses wake turbulence in stable conditions and increases the velocity and power deficits.

6. CONCLUSIONS AND DISCUSSION

It has been shown that the wind speed deficits obtained from the Jensen wake model for a single wind turbine, as function of the relative wind direction, depend on how we observe wakes. Results are different when considering that the deficits are observed by a point measurement, say a mast, compared with those when observed by a second turbine due to partial wake interaction. Therefore, for the 'turbine–turbine' case, the shape of the wind speed ratio is different compared with the original shape of the wind speed deficit obtained with the Jensen wake model.

Based on a simple relation between the TI and the mean wind speed of the free inflow, the wake decay coefficient of the Jensen wake model was expressed as a function of the height, roughness and atmospheric stability and, thus, of atmospheric turbulence. The relation between the TI, height and roughness (used to parameterize the wake decay coefficient) was shown to hold when analyzing met observations over a flat and nearly homogeneous terrain up to a height of 40 m and for a range of atmospheric stability conditions.

Wind Energ. 2016; **19**:763–776 © 2015 The Authors. *Wind Energy* published by John Wiley & Sons Ltd.
DOI: 10.1002/we

Although the 'direct' wind speed (or power) deficit from the Jensen wake model is constant across the width of the wake, it was shown that the wake deficits can become Gaussian with the maximum wind speed deficits lower and wakes wider than those from the 'direct' Jensen-like wake results. This is achieved through averaging of the simulation's output in a similar fashion to that in which the wake cases are observed, while partly accounting for the uncertainty in the wind direction using a Gaussian distribution that resembles the observed variability in the wind direction. For a typical wind farm, we should aim at measuring not only the distribution of the wind direction within the averaging period (which is typically 10 min, but as turbines react to wind changes much faster, then perhaps 1 min average will be even more appropriate) but also the distribution of wind direction changes between the averaging periods and that between turbines. van der Laan *et al*.[29] shows how to account practically for the uncertainty in the wind direction.

Further, we demonstrated the ability of an engineering wind farm wake model based on the Jensen wake model to simulate the single and double Sexbierum wake cases outperforming (for these particular cases) two more advanced ones: a linearized CFD model, Fuga, and a nonlinear CFD RANS wake model that uses a modified k-ε turbulence model. It was shown that the wake decay coefficient for these simulations should be lower ($k_w = 0.038$) than the value recommended by WAsP ($k_w = 0.075$) when accounting for atmospheric stability during both campaigns, as the observed TI is too low compared with that estimated from surface layer parameters assuming a neutral atmosphere.

The wake decay coefficient is the only adjustable parameter of the Jensen-based wake models (wind direction variability and uncertainty, which are also adjustable, can be accounted for as part of the post-processing). We show that this coefficient can be parameterized within the surface layer over a flat and homogeneous terrain. Although these conditions are rather 'ideal', results from the model described here using the parameterizations in equations (4) and (6) agree well with the WakeBench benchmark cases at Horns Rev I,[32] an offshore farm comprising turbines with a hub height of 70 m. We expect that it can also be used to accurately predict large turbine wake deficits, particularly under unstable and neutral conditions, as under these regimes, the surface layer can easily extend up to $\approx$ 100–200 m in middle latitudes. Also, atmospheric stability was accounted for in the k_w value in Peña *et al*.[6] for data from the Horns Rev I wind farm. A recent study showing, indirectly, the dependency on TI of k_w is that of Nygaard.[33] He showed very good agreement between a Jensen-like wind farm wake model and data from a northwest-southeast row with up to 20 turbines within the London array wind farm. He used a wake decay coefficient of 0.04, filtered data with wind speeds about 9 m s^{-1} and showed that at this wind speed, the observed TI was about 7%. He showed poorer agreement of the model (the simulated power ratios are not that low as those of the data) for a southwest-northwest row with up to 12 turbines using $k_w = 0.04$, although he showed that for that particular row, the observed TI was lower than 5%. Following our approach, a lower wake decay should be used for this second case, which will result in deeper deficits.

Jensen-based wake models are inherently not suited to study the wake characteristics in detail, for which more advanced models should be used. Here, we show that simple models can predict wake deficits accurately, now in a more transparent fashion as the wake coefficient can be parameterized. This is very important to address current challenges in wind farm optimization, as such simple models can be used during the first phase of wind farm layout design due to their efficiency, perhaps followed by a detailed CFD-based analysis. The model here described takes $\approx$74 s to estimate the annual energy production of an 80 turbine wind farm based on met data collected hourly over 1 year.

ACKNOWLEDGEMENTS

Funding from the EERA DTOC project (contract FP7-ENERGY-2011/n 282797) is acknowledged. This work is carried out as part of the IEA-WakeBench research collaboration project partly funded by EUDP WakeBench (contract 64011-0308).

REFERENCES

1. Jensen NO, *A note on wind generator interaction*, Technical Report Risoe-M-2411(EN), Risø National Laboratory, Roskilde, 1983.
2. Katic I, Højstrup J, Jensen NO. A simple model for cluster efficiency. *Proceedings of the European Wind Energy Association Conference & Exhibition*, Rome, 1986; 407–410.
3. Mortensen NG, Heathfield DN, Myllerup L, Landberg L, Rathmann O, *Getting started with WAsP 9*, Technical Report Risø-I-2571(EN), Risø National Laboratory, Roskilde, 2007.
4. Nielsen P, *Case studies calculating wind farm production*, Technical Report, EMD Energi- og Miljødata, Aalborg, 2002.
5. Gaumond M, Rethoré PE, Ott S, Peña A, Bechmann A, Hansen KS. Evaluation of the wind direction uncertainty and its impact on wake modelling at the Horns Rev offshore wind farm. *Wind Energy* 2014; **17**: 1169–1178.
6. Peña A, Réthoré P-E, Rathmann O. Modeling large offshore wind farms under different atmospheric stability regimes with the park wake model. *Renewable Energy* 2014; **70**: 164–171.

7. Ott S, Berg J, Nielsen M, *Linearised CFD models for wakes*, Technical Report Risø–R–1772(EN), Risø National Laboratory for Sustainable Energy, Roskilde, 2011.
8. Gaumond M, *Evaluation and benchmarking of wind turbine wake models*, Technical Report Master Thesis, DTU Wind Energy, Roskilde, 2012.
9. Sørensen NN, *General purpose flow solver applied to flow over hills*, Technical Report Risø-R-827(EN), Risø National Laboratory, Roskilde, 2003.
10. Troldborg N, *Actuator line modeling of wind turbine wakes*, Technical Report PhD Thesis, Technical University of Denmark, Lyngby, 2008.
11. Wan C, Wang J, Yang G, Gu H, Zhang X. Wind farm micro-siting by Gaussian particle swarm optimization with local search strategy. *Renewable Energy* 2012; **48**: 276–286.
12. Peña A, Rathmann O. Atmospheric stability-dependent infinite wind-farm models and the wake-decay coefficient. *Wind Energy* 2014; **17**: 1269–1285.
13. Frandsen S. On the wind speed reduction in the center of large clusters of wind turbines. *Journal of Wind Engineering and Industrial Aerodynamics* 1992; **39**: 251–265.
14. Stull RB. *An Introduction to Boundary Layer Meteorology*. Kluwer Academic Publishers: Dordrecht, 1988.
15. Obukhov AM. Turbulence in an atmosphere with a non-uniform temperature. *Boundary-Layer Meteorology* 1971; **2**: 7–29.
16. Peña A, Gryning SE. Hasager CB. Measurements and modelling of the wind speed profile in the marine atmospheric boundary layer. *Boundary-Layer Meteorology* 2008; **129**: 479–495.
17. Peña A, Gryning SE. Hasager CB. Comparing mixing-length models of the diabatic wind profile over homogeneous terrain. *Theoretical and Applied Climatology* 2010; **100**: 325–335.
18. Holtslag AAM. Estimates of diabatic wind speed profiles from near-surface weather observations. *Boundary-Layer Meteorology* 1984; **29**: 225–250.
19. Panofsky HA, Dutton JA. *Atmospheric Turbulence*. John Wiley & Sons: New York, 1984.
20. Peña A, Gryning SE. Mann J. On the length-scale of the wind profile. *Quarterly Journal of the Royal Meteorological Society* 2010; **136**: 2119–2131.
21. Peña A, Floors R, Gryning S.-E. The Høvsøre tall wind-profile experiment: a description of wind profile observations in the atmospheric boundary layer. *Boundary-Layer Meteorology* 2014; **150**: 69–89.
22. Peña A, *Sensing the wind profile*, Technical Report Risø-PhD-45(EN), Risø DTU, Roskilde, 2009.
23. Peña A, Gryning SE. Mann J, Hasager CB. Length scales of the neutral wind profile over homogeneous terrain. *Journal of Applied Meteorology and Climatology* 2010; **49**: 792–806.
24. Peña A, Gryning SE, Hahmann AN. Observations of the atmospheric boundary layer height under marine upstream flow conditions at a coastal site. *Journal of Geophysical Research-Atmospheres* 2013; **118**: 1924–1940.
25. Peña A, Floors R, Wagner R, Courtney MS, Gryning SE, Sathe A, Lars?n XG, Hahmann AN, Hasager CB. Ten years of boundary-layer and wind-power meteorology at Høvsøre, Denmark. *Boundary-Layer Meteorology* 2015. In review.
26. Gryning SE, Batchvarova E, Brümmer B, Jørgensen H, Larsen S. On the extension of the wind profile over homogeneous terrain beyond the surface layer. *Boundary-Layer Meteorology* 2007; **124**: 251–268.
27. van der Laan MP, Sørensen NN, Réthoré PE, Mann J, Kelly MC, Troldborg N, Schepers JG, Machefaux E. An improved k-ε model applied to a wind turbine wake in atmospheric turbulence. *Wind Energy* 2015; **18**: 889–907.
28. van der Laan MP, Sørensen NN, Réthoré PE, Mann J, Kelly MC, Troldborg N. The k-ε-f_p model applied to double wind turbine wakes using different actuator disk force methods. *Wind Energy* 2014. DOI: 10.1002/we.1816.
29. van der Laan MP, Sørensen NN, Réthoré PE, Mann J, Kelly MC, Troldborg N, Hansen KS, Murcia JP. The k-ε-f_p model applied to wind farms. *Wind Energy* 2014. DOI: 10.1002/we.1804.
30. Cleijne JW, *Results of the Sexbierum wind farm; double wake measurements*, Technical Report 92-388, TNO Environmental and Energy Research, Apeldoorn, Netherlands, 1992.
31. Cleijne JW, *Results of the Sexbierum wind farm; single wake measurements*, Technical Report 93-082, TNO Environmental and Energy Research, Apeldoorn, Netherlands, 1993.
32. Peña A, Réthoré PE, Hasager CB, Hansen K, *Results of wake simulations at the Horns Rev I and Lillgrund wind farms using the modified Park model*, Technical Report DTU Wind Energy-E-Report-0026(EN), DTU Wind Energy, Roskilde, 2013.
33. Nygaard NG. Wakes in very large wind farms and the effect of neighbouring wind farms. *Journal of Physics Conference Series* 2014; **524**: 012162 (10 pp).